Multiset-Based Image Segmentation

Luciano da Fontoura Costa
luciano@ifsc.usp.br

São Carlos Institute of Physics – DFCM/USP

14th Nov 2021

Abstract

Given an image, the identification of its constituent regions and components represents of the most challenging tasks in image analysis and pattern recognition, commonly known as image segmentation. In the present work, we show how recently developed concepts and methods based on the real-valued Jaccard and coincidence methods can be applied in order to achieve effective image segmentation. These concepts and methods are largely related to the generalization of multisets to real, possibly negative multiplicities. The two aforementioned coincidence indices are applied to quantify, in a strict and controllable manner, the similarity between every pair of pixes, yielding a respective complex network representation with enhanced modular structure. A parameter controlling the relative influence of pairs of pixels with the same or opposite signs on the overall result allows the selection of a suitable segmentation, which is then performed by using standard community finding algorithms.

'A picture is worth what we can understand from it.'

LdaFC

1 Introduction

Image segmentation, namely the identification of the several regions and components of an image (e.g. [1, 2]), corresponds to one of the most challenging operations in the areas of image analysis, computer vision, pattern recognition and artificial intelligence.

By extending multisets (e.g. [3, 4, 5, 6, 7, 8]) to real, possibly negative values [9, 10, 11], it has been possible to derive a respectiveliy generalized Jaccard similarity index [12, 13]. Though extensively used for binary and categorical data, this index had not been commonly applied considering negative multiplicities. Given that the Jaccard index is not able to take into account the relative interiority between the compared sets, a respective extension has been proposed [9] which also takes into account the interiority (or overlap [14]) index. More specifically, this gives rise to the *coincidence index* [9], corresponding to the product of the Jaccard and interiority indices.

The real-valued Jaccard and coincidence indices have been shown to be closely related to the generalized Kronecker delta function [15, 11, 16], to the point of converging steadily to it when the numerator in the definition of the real-valued Jaccard index is taken to an increasing odd non-negative integer power [16].

The specific way in which the real-valued Jaccard and coincidence indices work, namely penalizing in a more effective manner values that are relatively more distinct one another than typically performed by product-based indices including the cosine similarity and Pearson correlation, the two aforementioned multiset indices pave the way to impressive performance in a wide range of tasks involving the quantification of similarities, including but not being limited to: template matching [17], neuronal pattern recognition [18], hierarchical clustering [19], and transforming datasets into networks with detailed interconnectivity and enhanced modularity [20].

In the present work, we extend the application of the two considered multiset indices, namely the real-valued Jaccard and coincidence methods, to the particularly challenging task of *image segmentation* [1, 2], with impressive results.

We start by presenting the real-valued Jaccard and coincidence methods, and then illustrate their respective potential for image segmentation.

2 The Real-Valued Jaccard and Coincidence Indices

Let the following binary operations (in the sense of taking two operands) related to multisets extended to real,

possibly negative multiplicities [9, 10, 11, 16]:

$$f \sqcap g = \int_S s_{fg} \min\{s_f f, s_g g\} \, dz \tag{1}$$

$$f \sqcup g = \int_S s_{fg} \max\{s_f f, s_g g\} \, dz \tag{2}$$

$$f \sqcap_- g = \int_S |s_f - s_g|/2 \min\{s_f f, s_g g\} \, dz \tag{3}$$

$$f \sqcap_+ g = \int_S |s_f + s_g|/2 \min\{s_f f, s_g g\} \, dz \tag{4}$$

$$f \tilde{\sqcap} g = \int_S \min\{s_f f, s_g g\} \, dz \tag{5}$$

$$f \tilde{\sqcup} g = \int_S \max\{s_f f, s_g g\} \, dz \tag{6}$$

where $f = f(z)$ and $g = g(z)$ are real valued functions or fields, and $s_f = sign(f(z))$, $s_y = sign(g(z))$, and $s_{fg} = s_f s_g$. The extension to discrete functions and fields is immediate. Observe that the above formulation also takes into account the generalization of multisets to real-valued functions and fields [9, 10, 11, 16]. The operations 9 and 1 had also been considered previously, respectively in [21] and [22], in the context of being possibly analogous to the inner product in the L1 space.

The above binary operations arise naturally when multisets are extended to possibly negative multiplicities as a consequence of the several ways in which combinations of the sign pairwise values can be taken while calculating the respective operations, through functionals over the free variable z. In particular, Equation 1 has been verified to correspond to the intersection between two signed multisets, required so that $\Phi \sqcap A = \Phi$, with Φ being the empty multiset and A being a generic multiset.

Observe that the terms s_{xy}, $|s_f + s_g|$, and $|s_f - s_g|$, here called *conjoint sign functions*, act as selectors of the portions of the functions to be integrated according to respective sign rules. For instance, in the case of Equation 8, only the intervals of z in which the signs of the two functions are opposite are considered in the respective integration required by the respective functional.

Given the above multiset binary operations, we can now define the *real-valued Jaccard index* [9, 10, 15, 11] between two functions (or multisets) f and g as:

$$\mathcal{J}_R(f,g) = \frac{\int_S s_{fg} \min\{s f_f, s_g g\} \, dz}{\int_S \max\{s f_f, s_g g\} \, dx} = \frac{f \sqcap g}{f \tilde{\sqcup} g} \tag{7}$$

where S is the *combined support* underlying both f and g.

In order to have a parameter controlling the respective contributions of the pairs of values with the same or opposite signs, we make:

$$s_- = s_-(f,g) = \int_S |s_f - s_f| \min\{s_f f, s_g g\} \, dz \tag{8}$$

$$s_+ = s_+(f,g) = \int_S |s_f + s_f| \min\{s_f f, s_g g\} \, dz \tag{9}$$

$$\tag{10}$$

and then take:

$$s_\pm(f,g,\alpha) = [\alpha] \, s_- - [1-\alpha] \, s_+ \tag{11}$$

which yields the following α-controlled real-valued Jaccard index:

$$\mathcal{J}_R(f,g) = \frac{\int_S s_\pm(f,g,\alpha) \, dz}{\int_S \max\{s f_f, s_g g\} \, dx} \tag{12}$$

Because the Jaccard index is not able to take into account the relative interiority between the two functions [9], it has been complemented by considering the interiority index (also overlap [14]). When adapted to real, possibly negative values, the interiority index becomes:

$$\mathcal{I}_R(f,g) = \frac{\int_S \min\{s f_f, s_g g\} \, dz}{\min\{S_f, S_g\}} = \frac{f \sqcap g}{\min\{S_f, S_g\}} \tag{13}$$

where:

$$S_f = \int_S s_f f(z) dz \tag{14}$$

$$S_g = \int_S s_g g(z) dz \tag{15}$$

The *coincidence index* can now be expressed [9, 10, 15, 11] as corresponding to the product between the real-valued Jaccard and interiority indices:

$$\mathcal{C}_R(f,g) = \frac{[f \sqcap g] \, [f \tilde{\sqcap} g]}{[f \tilde{\sqcup} g] \min\{S_f, S_g\}} \tag{16}$$

or, in expanded form:

$$\mathcal{C}_R(f,g) = \\ = \frac{\left[\int_S s_\pm(f,g,\alpha) dz\right] \left[\int_S \min\{s_f f, s_g g\} \, dz\right]}{\left[\int_S \max\{s_f f, s_g g\} \, dz\right] \left[\min\{S_f, S_g\}\right]} \tag{17}$$

3 Multiset Image Segmentation

Though we will henceforth limit our attention to gray-level images, all the proposed concepts and methods can be immediately extended to colored, multi-spectral or even multi-dimensional images.

A gray-level image (e.g. [1, 2]) can be understood as a matrix $A[i,j]$, with $i = 1, 2, \ldots, N_i$ and $j = 1, 2, \ldots, N_j$, therefore having dimension $N_x \times N_y$. Each of the elements

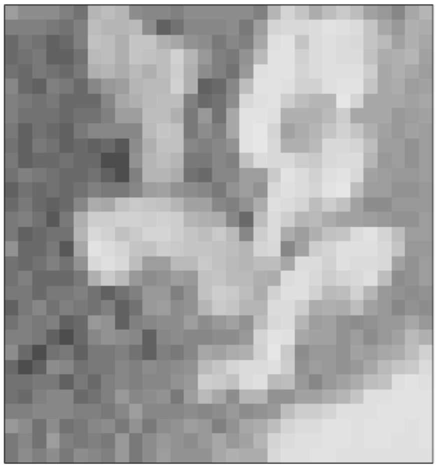

Figure 1: A small gray-scale image considered for illustrating the multiset-based segmentation method.

of the image matrix are called *pixels*, their value being related to the respective level of luminosity.

Figure 1 illustrates a small gray-level image of a flower.

Before the coincidence-based methodology proposed in [20] can be applied as a means to transform the image into a network with enhanced modularity, it is first necessary to associate suitable features to each of its constituent pixels. Among the several (actually infinite) possibilities of doing so, here we adopt the positions (or coordinates) i and j of the pixel, its intensity value $A\left[i,j\right]$ as well as the average intensity in a square region of radius 1 centered at the pixel position (i.e. a 3×3 window).

Therefore, each of the image pixels becomes associated to the following feature vector:

$$\vec{f}_{A[i,j]} = \left[i, j, A\left[i,j\right], W\left[i,j\right]\right] \tag{18}$$

where $W\left[i,j\right]$ corresponds to the average pixel value in the 3×3 windos. Other features can be eventually assigned, including those related to color, texture, etc. Another interesting possibility is to take some transformation of the coordinate values i and j, e.g. by weighting them according to density, homogeneity, etc.

In order to get a more commensurate, non-dimensional representation of the above features, we perform their respective *statistical standardization*, which consists of making:

$$\tilde{f}_i = \frac{f_i - \mu_{f_i}}{\sigma_{f_i}} \tag{19}$$

where μ and σ stand for the respective mean and standard deviation [2, 23]. After standardization, the features will have null means and unit standard deviation, and most of the resulting values will be comprised in the interval $[-2, 2]$.

Figure 2 depicts the image segmentation obtained by using the fast greedy method [24] considering $\alpha = 0.5$ and $T = 0.7$.

Figure 2: The segmentation of the image in Fig. 1 by using the proposed methodology considering $\alpha = 0.5$ and $T = 0.7$.

The modular network obtained from the original gray-level image considering $\alpha = 0.5$ and $T = 0.7$ is shown in Figure 3. Each of the obtained communities gives rise to a respective segmented region shown in different arbitrary colors in Figure 2. The compact cluster at the left-hand side corresponds to the null border of the image required for the calculation of the average pixel intensities within the window 3×3.

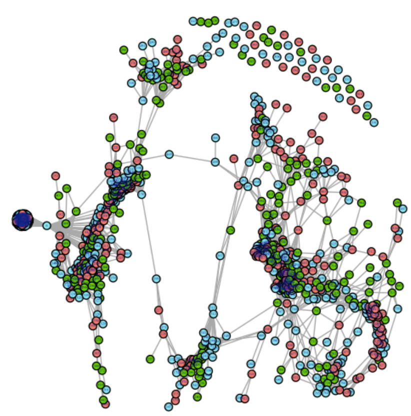

Figure 3: The modular network obtained for the considered image. Each of the communities define a respective segmented image region, shown in different arbitrary colors in Fig. 2.

Figure 4 depicts the histogram of coincidence values obtained for the considered example, which define a smooth distribution with a peak near 0.

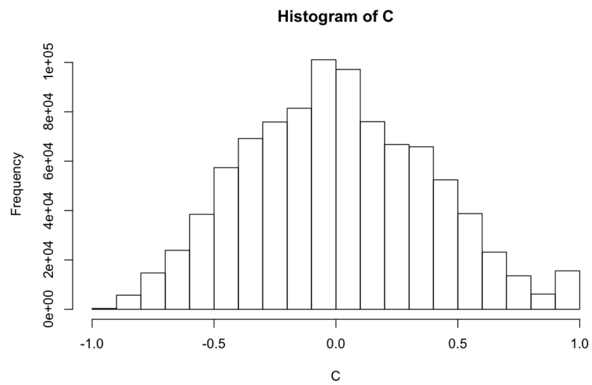

Figure 4: The segmentation of the image in Fig. 1 by using the proposed methodology considering $\alpha = 0.5$ and $T = 0.7$.

4 Concluding Remarks

Image segmentation has represented a substantial challenge in the areas of image processing, image analysis, computer vision, pattern recognition and artificial intelligence.

In the present work, we proposed a methods for image segmentation that is based on the representation of datasets into networks with detailed and enhanced modularity obtained by using the coincidence index [20]. Features are extracted and associated to each of the image pixels, including their position and local luminosity. These datasets are then transformed into respective networks. A suitable value of the parameters α is then selected so as to make the communities well-defined, which is then followed by the application of some community finding methodology.

The impressive potential of the reported methodology for image segmentation is illustrated respectively to a simple gray-level image.

Several further developments are possible, including but not being limited to the following possibilities: (i) to consider larger and diverse images; (ii) to verify the effect of other possible features for characterization of each pixel including those related to color and texture; (iii) develop automated methods for selecting the a proper value of α, e.g. by considering entropy maximization; and (iv) to apply the methodology to multi-spectral and multidimensional images. Related research is being developed and results are expected to be communicated opportunely.

Acknowledgments.

Luciano da F. Costa thanks CNPq (grant no. 307085/2018-0) and FAPESP (grant 15/22308-2).

References

[1] R. J. Schalkoff. *Digital Image Processing and Computer Vision*. Wiley, 1989.

[2] L. da F.Costa. *Shape Classification and Analysis: Theory and Practice*. CRC Press, Boca Raton, 2nd edition, 2009.

[3] J. Hein. *Discrete Mathematics*. Jones & Bartlett Pub., 2003.

[4] D. E. Knuth. *The Art of Computing*. Addison Wesley, 1998.

[5] W. D. Blizard. Multiset theory. *Notre Dame Journal of Formal Logic*, 30:36—66, 1989.

[6] W. D. Blizard. The development of multiset theory. *Modern Logic*, 4:319–352, 1991.

[7] P. M. Mahalakshmi and P. Thangavelu. Properties of multisets. *International Journal of Innovative Technology and Exploring Engineering*, 8:1–4, 2019.

[8] D. Singh, M. Ibrahim, T. Yohana, and J. N. Singh. Complementation in multiset theory. *International Mathematical Forum*, 38:1877–1884, 2011.

[9] L. da F. Costa. Further generalizations of the Jaccard index. https://www.researchgate.net/publication/355381945_Further_Generalizations_of_the_Jaccard_Index, 2021.

[10] L. da F. Costa. Multisets. https://www.researchgate.net/publication/355437006_Multisets, 2021.

[11] L. da F. Costa. Generalized multiset operations. https://www.researchgate.net/publication/356191988_Generalized_Multiset_Operations, 2021. [Online; accessed 10-Nov-2021].

[12] P. Jaccard. Distribution de la flore alpine dans le bassin des dranses et dans quelques régions voisines. *Bulletin de la Société vaudoise des sciences naturelles*, 37:241–272, 1901.

[13] Wikipedia. Jaccard index. https://en.wikipedia.org/wiki/Jaccard_index. [Online; accessed 10-Oct-2021].

[14] M. K. Vijaymeena and K. Kavitha. A survey on similarity measures in text mining. *Machine Learning and Applications*, 3(1):19–28, 2016.

[15] L. da F. Costa. On similarity. https://www.researchgate.net/publication/355792673_On_Similarity, 2021.

[16] L. da F. Costa. The classic cross-correlation and the real-valued jaccard and coincidence indices. https://www.researchgate.net/publication/356490253_The_Classic_Cross-Correlation_and_the_Real-Valued_Jaccard_and_Coincidence_Indices, 2021.

[17] L. da F. Costa. Comparing cross correlation-based similarities. https://www.researchgate.net/publication/355546016_Comparing_Cross_Correlation-Based_Similarities, 2021.

[18] L. da F. Costa. Multiset neurons. https://www.researchgate.net/publication/356042155_Common_Product_Neurons, 2021.

[19] L. da F. Costa. Real-valued jaccard and coincidence based hierarchical clustering. https://www.researchgate.net/publication/355820021_Real-Valued_Jaccard_and_Coincidence_Based_Hierarchical_Clustering, 2021.

[20] L. da F. Costa. Coincidence complex networks. https://www.researchgate.net/publication/355859189_Coincidence_Complex_Networks, 2021.

[21] B. Mirkin. *Mathematical Classification and Clustering*. Kluwer Academic Publisher, Dordrecth, 1996.

[22] C. E. Akbas, A. Bozkurt, M. T. Arslan, H. Aslanoglu, and A. E. Cetin. L1 norm based multiplication-free cosine similiarity measures for big data analysis. In *IEEE IWCIM*, France, Nov. 2014.

[23] R. A. Johnson and D.W. Wichern. *Applied multivariate analysis*. Prentice Hall, 2002.

[24] A. Clauset, M. E. J. Newman, and C. Moore. Finding community structure in very large networks. *Phys. Rev. E*, 70:066111, 2004.